Copper-based coordination polymers from thiophene and furan dicarboxylates with high isosteric heats of hydrogen adsorption†

Jie Yang,[ab] Martin Lutz,[c] Anna Grzech,[d] Fokko M. Mulder[d] and Theo J. Dingemans*[b]
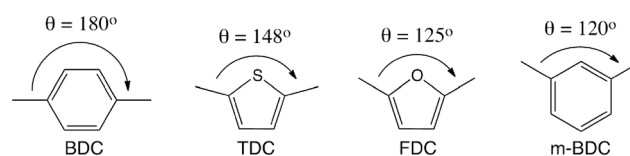
Self-assembled Cu-based coordination polymers derived from thiophene-2,5-dicarboxylic acid (Cu-TDC) and furan-2,5-dicarboxylic acid (Cu-FDC) were synthesized via a solvothermal method and their H_2 adsorption behaviour was investigated and contrasted with isophthalic acid (Cu-m-BDC) and terephthalic acid (Cu-BDC) derivatives. Both heterocyclic-based coordination polymers exhibit low surface areas (<300 m^2 g^{-1}) upon activation but unusually high isosteric heats of hydrogen adsorption (7.5–9.2 kJ mol^{-1}). Hydrogen uptake values of 0.64–0.75 wt% (77 K and 1 bar) were recorded and these high uptake values are attributed to the optimal pore size (5.4–8 Å) and the polarizability of the 5-membered heterocycles.

Introduction

Metal–organic coordination polymers are promising candidates for hydrogen storage, gas separation and optoelectronic applications. In these materials, polyfunctional organic ligands form coordination bonds with multiple metal atoms, which may extend into one-, two-, or three-dimensional polymeric structures.[1,2] Benzenecarboxylic acids and nitrogen-based heterocyclic carboxylic acids have been well documented as useful building blocks for the construction of a wide variety of metal–organic coordination polymers.[3] More interestingly, introducing oxygen- or sulphur-containing heterocycles would endow metal–organic coordination polymers with unique physical and chemical properties.[4] To date, a systematic study on the hydrogen storage properties of heterocyclic-based metal–organic coordination polymers has not been reported.

Thiophene-2,5-dicarboxylic acid (H$_2$TDC) and furan-2,5-dicarboxylic acid (H$_2$FDC) are two basic representatives of the heterocyclic dicarboxylic acid family. Owing to the larger radius of the S atom, as compared to C, N, and O, its one pair of electrons can easily delocalize over the heterocyclic ring, and as a ligand thiophene-2,5-dicarboxylic acid exhibits good charge-transfer ability. Furan-2,5-dicarboxylic acid, on the other hand, is of interest for similar reasons but in particular because it is considered to be a bio-renewable building block in the formation of polymers from biomass. We have selected copper(II) as the cation because Jahn–Teller distortions will weaken the bonding of solvent molecules at the axial sites. The resulting open metal sites and the Cu$^{\delta+}$–O$^{\delta-}$ dipoles on the surface generated upon removal of these solvent molecules will result in an enhancement of the local interaction energy for hydrogen.[5] In the present work, we have synthesized Cu-based coordination polymers derived from thiophene-2,5-dicarboxylic acid (H$_2$TDC) and furan-2,5-dicarboxylic acid (H$_2$FDC). Cu-based coordination polymers based on terephthalic acid (Cu-BDC) and isophthalic acid (Cu-m-BDC) were also prepared as reference materials because they don't contain a transverse dipole moment and this series allows us to investigate the role of the exocyclic bond angle (θ) of the dicarboxylate linker shown in Scheme 1. Herein we report on the structural characteristics, stability and hydrogen storage properties of this series of Cu-based coordination polymers.

[a] College of Mathematics and Physics, Shanghai University of Electric Power, Shanghai, 200090, PR China
[b] Faculty of Aerospace Engineering, Delft University of Technology, Kluyverweg 1, Delft, The Netherlands. E-mail: t.j.dingemans@tudelft.nl; Fax: +31(0)152784472; Tel: +31(0)152784520
[c] Crystal and Structural Chemistry, Bijvoet Center for Biomolecular Research Faculty of Science, Utrecht University, Padualaan 8, 3584 CH Utrecht, The Netherlands
[d] Department of Chemical Engineering, Faculty of Applied Sciences, Delft University of Technology, Mekelweg 15, 2629 JB Delft, The Netherlands. E-mail: f.m.mulder@tudelft.nl; Fax: +31(0)152783803; Tel: +31(0)152784870
† Electronic supplementary information (ESI) available: characterization data including X-ray crystal structures, TG curves and hydrogen isotherms. CCDC 956646–956648. For ESI and crystallographic data in CIF or other electronic format see DOI: 10.1039/c4ce00145a

Scheme 1 The exocyclic bond angle (θ) of the dicarboxylate linker units.

Experimental

Materials

Cu(NO$_3$)$_2$·2.5H$_2$O (Acros, 97%), thiophene-2,5-dicarboxylic acid (H$_2$TDC, George Uh4 Co., Inc.), furan-2,5-dicarboxylic acid (H$_2$FDC, TCI, 98%), isophthalic acid (*m*-H$_2$BDC, Acros, 98%), terephthalic acid (H$_2$BDC, BP, >99%), *N*,*N*′-dimethylformamide (DMF, Acros), chloroform (CHCl$_3$), absolute ethanol (EtOH), and benzene were used as received. Isophthalic acid was recrystallized from EtOH.

Synthesis

Synthesis of Cu-TDC. In a 20 mL vial, 23.7 mg (0.10 mmol) of Cu(NO$_3$)$_2$·2.5H$_2$O and 23.0 mg (0.13 mmol) of thiophene-2,5-dicarboxylic acid were dissolved in DMF/H$_2$O/EtOH (1.5 mL/0.25 mL/0.5 mL). The vial was placed into a preheated oven and kept at 80 °C for 24 h. Blue crystals were collected and washed with DMF and EtOH, then vacuum dried overnight at 25 °C. The product (23.5 mg) was labeled Cu-TDC and stored in a glove box.

Synthesis of Cu-FDC. In a 20 mL vial, 22.3 mg (0.096 mmol) of Cu(NO$_3$)$_2$·2.5H$_2$O and 21.4 mg (0.14 mmol) of furan-2,5-dicarboxylic acid were dissolved in DMF/H$_2$O/EtOH (1.5 mL/0.5 mL/0.5 mL). The vial was placed into a preheated oven and kept at 80 °C for 24 h. Blue crystals were filtered and washed with DMF and EtOH, then vacuum dried overnight at 25 °C. The product (25.0 mg) was labeled Cu-FDC and stored in a glove box.

Synthesis of Cu-BDC. 0.6958 g (3.0 mmol) of Cu(NO$_3$)$_2$·2.5H$_2$O and 0.4979 g of terephthalic acid (3.0 mmol) were dissolved in 60 mL of DMF. The solution was placed in a preheated oven at 110 °C for 36 h. The product was collected as a blue powder and washed with DMF (2 × 30 mL), followed by heating at 60 °C under vacuum overnight. The product (0.54 g) was labeled Cu-BDC and stored in a glove box.

Synthesis of Cu-*m*-BDC. 0.5598 g (3.37 mmol) of isophthalic acid and 0.7601 g (3.27 mmol) of Cu(NO$_3$)$_2$·2.5H$_2$O were dissolved in a mixed solution of DMF–EtOH (60 mL/20 mL). The solution was placed into a preheated oven at 80 °C for 24 h. The blue crystals were washed with DMF–EtOH mixture (3:1) (3 × 20 mL) and dried at r.t. under vacuum for 7 h. The product (0.42 g) was labeled Cu-*m*-BDC and stored in a glove box.

Activation. The samples were activated using the following methods. A – CHCl$_3$-exchange (SE(CHCl$_3$)): under an inert atmosphere, Cu-TDC was extracted three times with fresh CHCl$_3$ (2 mL for 15 h, 2 mL for 9 h, 2 mL for 15 h) and dried under vacuum at room temperature overnight and at 60 °C for 3 days. The activated samples were denoted as Cu-TDC-SE(CHCl$_3$). The CHCl$_3$-exchange was also employed for activating the Cu-FDC and Cu-*m*-BDC samples. The resulting samples were denoted as Cu-FDC-SE(CHCl$_3$) and Cu-*m*-BDC-SE(CHCl$_3$), respectively. B – EtOH-exchange (SE(EtOH)): under an inert atmosphere, 200 mg of Cu-*m*-BDC or Cu-BDC was extracted two times with absolute EtOH (20 mL for 15 h, 20 mL

for 14 h) and dried under vacuum at room temperature overnight and at 45 °C for 20 h. The activated samples were denoted as Cu-*m*-BDC-SE(EtOH) and Cu-BDC-SE(EtOH), respectively. C – Freeze-drying (FD): about 400 mg of a fresh sample was placed in a Schlenk tube and washed with CH$_2$Cl$_2$ (10 mL × 3) and benzene (8 mL × 2), followed by immersing in 10 mL of benzene overnight. The tube was placed into an ice-water bath (0 °C). After three freeze–thaw cycles, the sample was evacuated in an ice-water bath for 24 h. The sample was kept under vacuum at room temperature for 24 h and at 60 °C for 24 h. The samples activated *via* this freeze-drying process were labeled Cu-TDC-FD, Cu-FDC-FD and Cu-*m*-BDC-FD.

Characterization

Single-crystal X-ray structure determination of Cu-TDC. C$_9$H$_9$CuNO$_5$S + disordered solvent, Fw = 306.77.‡ Sample appearance and dimensions: blue block, 0.41 × 0.39 × 0.26 mm^3. Trigonal, *R*$\bar{3}$*c* (no. 167), *a* = *b* = 20.0402(6), *c* = 41.6541(13) Å, *V* = 14 487.5(8) Å^3, *Z* = 36, *D$_x$* = 1.266 g cm^{-3},‡ *μ* = 1.49 mm^{-1}.‡ 62 951 reflections were measured on a Bruker Kappa ApexII diffractometer with a sealed tube and a Triumph monochromator (*λ* = 0.71073 Å) up to a resolution of (sin *θ*/*λ*)$_{max}$ = 0.65 Å^{-1} at a temperature of 150(2) K. Intensity data were integrated using the SAINT software.[6] Absorption correction and scaling were performed based on multiple measured reflections using SADABS (0.65–0.75 correction range).[7] 3715 reflections were unique (*R$_{int}$* = 0.026), of which 2649 were observed [*I* > 2*σ*(*I*)]. The structure was solved with direct methods using the program SHELXS-97 and refined with SHELXL-97 against *F*^{2} of all reflections.[8] Non-hydrogen atoms were refined with anisotropic displacement parameters. Hydrogen atoms were introduced in calculated positions and refined with a riding model. The crystal structure contains solvent accessible voids (5441 Å^3 per unit cell) filled with disordered solvent molecules. Their contribution to the structure factors was secured by back-Fourier transformation using the SQUEEZE routine in PLATON resulting in 1482 electrons per unit cell.[9] The *N*,*N*′-dimethylformamide ligand was refined with a disorder model. 182 parameters were refined with 54 restraints (concerning the disordered DMF). *R$_1$*/w*R$_2$* [*I* > 2*σ*(*I*)]: 0.0367/0.1204. *R$_1$*/w*R$_2$* (all refl.): 0.0473/0.1281. *S* = 1.141. Residual electron density is between −0.47 and 0.49 e Å^{-3}. Geometry calculations and checking for higher symmetry were performed using the PLATON program.[9]

Single-crystal X-ray structure determination of Cu-FDC. C$_{18}$H$_{12}$Cu$_3$O$_{18}$ + disordered solvent, Fw = 706.90.§ Sample appearance and dimensions: blue needle, 0.40 × 0.15 × 0.14 mm^3. Monoclinic, *C*2/*m* (no. 12), *a* = 18.9198(11), *b* = 18.8335(14), *c* = 12.6671(8) Å, *β* = 92.396(3)°, *V* = 4509.7(5) Å^3, *Z* = 4, *D$_x$* = 1.041 g cm^{-3},§ *μ* = 1.45 mm^{-1}.§ 75 193 reflections

---

‡ Derived values do not include the contribution of the disordered solvent molecules.

§ Derived values do not include the contribution of the disordered solvent molecules.

were measured on a Bruker Kappa ApexII diffractometer with a sealed tube and a Triumph monochromator ($\lambda = 0.71073$ Å) up to a resolution of $(\sin\theta/\lambda)_{\max} = 0.65$ Å^{-1} at a temperature of 150(2) K. The crystal was non-merohedrally twinned with a twofold rotation about $uvw = [-1,-1,2]$ as a twin operation. Intensity data were integrated using the Eval14 software[10] taking the twin relation into account. Absorption correction, scaling, and de-twinning were performed based on multiple measured reflections using TWINABS[7] (0.65–0.75 correction range). 5351 reflections were unique ($R_{\mathrm{int}} = 0.040$), of which 4804 were observed [$I > 2\sigma(I)$]. The structure was solved with direct methods using the program SHELXS-97 and refined with SHELXL-97 against F^2 of all reflections.[8] Non-hydrogen atoms were refined with anisotropic displacement parameters. Hydrogen atoms were introduced in calculated positions and refined with a riding model. The crystal structure contains solvent accessible voids (2650 Å^3 per unit cell) filled with disordered solvent molecules. Their contribution to the structure factors was secured by back-Fourier transformation using the SQUEEZE routine in PLATON resulting in 838 electrons per unit cell.[9] 181 parameters were refined with no restraints. R_1/wR_2 [$I > 2\sigma(I)$]: 0.0320/0.0835. R_1/wR_2 (all refl.): 0.0354/0.0850. $S = 1.040$. Residual electron density is between -0.50 and 2.39 e Å^{-3}. Geometry calculations and checking for higher symmetry were performed using the PLATON program.[9]

Single-crystal X-ray structure determination of Cu-m-BDC. C$_{222}$H$_{166}$Cu$_{24}$N$_{10}$O$_{120}$ + disordered solvent, Fw = 6418.60.¶ Sample appearance and dimensions: blue needle, 0.40 × 0.16 × 0.15 mm^3. Triclinic, $P\bar{1}$ (no. 2), $a = 21.4985(13)$, $b = 24.7145(14)$, $c = 24.8218(14)$ Å, $\alpha = 110.166(4)$, $\beta = 112.898(3)$, $\gamma = 102.544(2)°$, $V = 10\,420.7(11)$ Å^3, $Z = 1$, $D_x = 1.023$ g cm^{-3},¶ $\mu = 1.26$ mm^{-1}.¶ 86\,010 reflections were measured on a Bruker Kappa ApexII diffractometer with a sealed tube and a Triumph monochromator ($\lambda = 0.71073$ Å) up to a resolution of $(\sin\theta/\lambda)_{\max} = 0.56$ Å^{-1} at a temperature of 150(2) K. Intensity data were integrated using the Eval15 software.[11] Absorption correction and scaling were performed based on multiple measured reflections using SADABS[7] (0.66–0.74 correction range). 30\,432 reflections were unique ($R_{\mathrm{int}} = 0.038$), of which 20\,697 were observed [$I > 2\sigma(I)$]. The structure was solved using the program SHELXT and refined with SHELXL-2013 against F^2 of all reflections.[8] Non hydrogen atoms of the framework were refined with anisotropic displacement parameters. Coordinated solvent molecules (DMF, H$_2$O) were disordered on the same coordination site and were refined with isotropic displacement parameters. Hydrogen atoms were introduced in calculated positions and refined with a riding model. Hydrogen atoms of the water molecules were omitted. The crystal structure contains solvent accessible voids (4443 Å^3 per unit cell) filled with disordered solvent molecules. Their contribution to the structure factors was secured by back-Fourier transformation using the SQUEEZE routine in PLATON resulting in 1069 electrons per

unit cell.[9] 1613 parameters were refined with 190 restraints (concerning disordered DMF). R_1/wR_2 [$I > 2\sigma(I)$]: 0.0712/0.2220. R_1/wR_2 (all refl.): 0.0969/0.2456. $S = 1.057$. Residual electron density is between -0.80 and 1.69 e Å^{-3}. Geometry calculations and checking for higher symmetry were performed using the PLATON program.[9]

Powder XRD, elemental analysis, TGA, BET, and H$_2$ adsorption

XRD patterns of all samples were recorded using an X'Pert X-ray diffractometer operated at 45 kV and 40 mA with monochromatic Cu Kα radiation within a 2-theta range of 5–60°. IR spectra were collected using a PerkinElmer Spectrum 100 FT-IR Spectrometer. Elemental analyses were performed using a Thermo Scientific InterScience Flash 2000 Organic Elemental Analyzer. TGA curves were obtained using a PerkinElmer Pyris Diamond Thermogravimetric Differential Thermal/Analyzer. Samples were heated from room temperature to 600 °C with a heating rate of 10 °C min^{-1} under a dry air flow. The pore textural properties, including the BET surface area and pore volume, were recorded using a Micromeritics ASAP 2010 adsorption analyser at 77 K. Prior to the adsorption measurements, the samples were degassed *in situ* under vacuum at 50 °C (for the samples activated by solvent-exchange) or at 80 °C (for the samples activated by freeze-drying) overnight. The dead volume of the sample cell was determined in a separate experiment. *In situ* pretreatment coupled to a separate dead volume measurement after the analysis was employed in order to avoid the helium entrapment phenomenon. The weight of a sample obtained after the pretreatment was used in various calculations. BET surface areas were calculated in the adapted pressure range of $P/P_0 = 0.01$–0.1. Hydrogen storage measurements in the low-pressure range (<2 bar) were performed on a Sievert's setup at 77 K and 100 K. Prior to the measurement, the samples activated by solvent-exchange were pretreated under high vacuum (10^{-6} mbar) at 25 °C for 1 day. The samples activated by freeze-drying were pretreated under high vacuum (10^{-6} mbar) at 80 °C for 1 day. Hydrogen (ultra-high-purity grade, 99.999%) was additionally purified by leading it over a bed of zeolite spheres at 77 K before being loaded onto the samples. The pressure change was monitored and recorded after the hydrogen reservoir was connected to the sample holder. The samples were weighed in a glove box after the measurements for calculating the hydrogen uptake capacities. The amount of hydrogen stored in the dead volume was examined using sea sand as a reference. The hydrogen uptake capacities of all samples were obtained by subtracting the amount of hydrogen in the dead volume from the total amount of hydrogen released from the reservoir.

Results and discussion

Crystal structures

The structures of Cu-TDC (Fig. S1–S6 and Table S1–S3†), Cu-m-BDC (Fig. S7–S8†), and Cu-BDC are similar to those

---

¶ Derived values do not include the contribution of the disordered solvent molecules. They also do not include the H atoms of the water molecules.

reported before.[12–14] Their detailed structures were described in the ESI†.[15]

The new Cu-based coordination polymer composed of furan-2,5-dicarboxylate (Cu(FDC)(H$_2$O)) crystallizes in the monoclinic space group $C2/m$ (no. 12) with one Cu-center on a mirror plane and one Cu-center on a general position. The asymmetric unit contains 1.5 Cu^{2+} ions, 1.5 FDC ligands and 1.5 coordinated H$_2$O molecules (Fig. 1). Cu1 and water oxygen O1 are located on the mirror plane x, 0.5, z and oxygen O5 of a FDC ligand is located on the mirror plane x, 0, z. Due to the deprotonation of all carboxylates the FDC ligands are dianionic. The carboxylate groups are bridging two copper ions into a Cu$_2$O$_8$C$_4$ unit, which is similar to that in Cu-TDC. Because of the lower symmetry than that in Cu-TDC, there are two independent Cu$_2$O$_8$C$_4$ units with C_{2h} and C_i symmetry, respectively, and the Cu–Cu distances in Cu-FDC are 2.6518(6) and 2.6782(5) Å. A simplified representation of the cluster is shown in Fig. S9.† There are four carboxylate bridges for every Cu$_2$ unit. In the Cu-FDC structure, the sixth coordinated position at each Cu ion is occupied by a water molecule. The Cu–O distances of the water ligands are longer than the carboxylate distances. Both independent Cu centers are in distorted octahedral environments. Selected bond distances and angles are given in Table S4.†

The furan cores of the FDC ligands link the Cu$_2$ dimers into an infinite two-dimensional network in the crystallographic (2,0,1) plane (Fig. 2). The Cu ions occupy the corners of triangles. The Cu···Cu distances between the corners vary
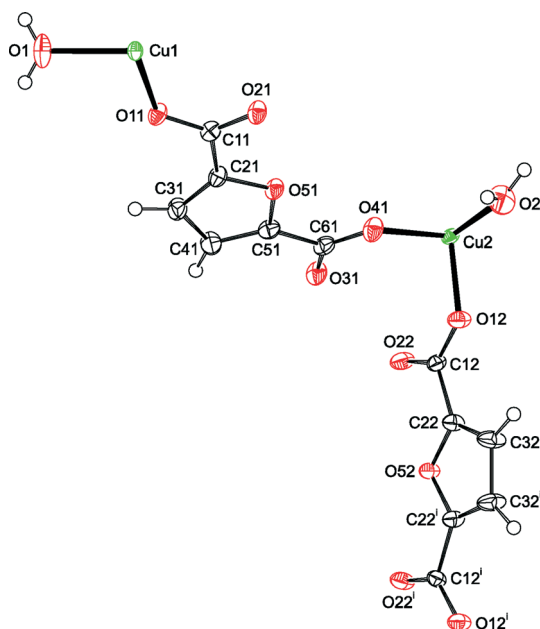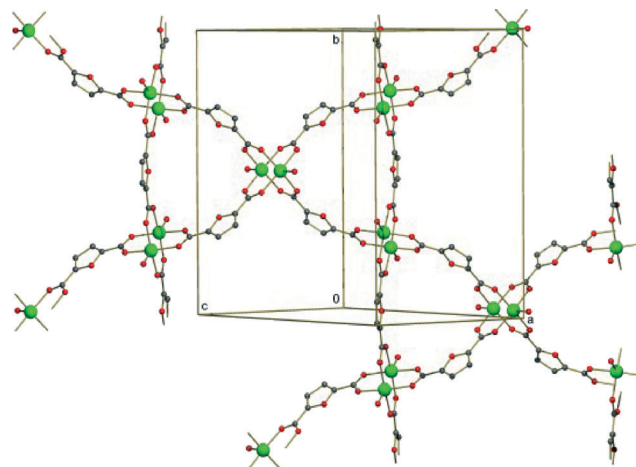

Fig. 2 An infinite two-dimensional coordination layer in the crystal structure of Cu-FDC. Hydrogen atoms are omitted for clarity.

between 8.2732(7) for Cu2···Cu1^i and 10.5170(8) Å for Cu2···Cu2^v (i: $-x$, y, $1 - z$; v: x, $-y$, z).

Cu-FDC contains coordinated water molecules, which can act as hydrogen bond donors. The acceptors for these hydrogen bonds are not part of the framework structure but are located in the solvent area. In the framework there is only one weak C–H···O hydrogen bond linking the stacked 2D layers. Furan carbon atom C32 is the donor of the hydrogen bond and carboxylate oxygen O11 is the acceptor (Fig. 3 and Table S5†).

The crystal structure of Cu-FDC contains large solvent accessible voids. PLATON calculates a volume percentage of ~58% for these voids (Fig. 4).

The exocyclic angles of m-H$_2$BDC, H$_2$FDC, H$_2$TDC, and H$_2$BDC are 120°, 125°, 148° and 180°, respectively. Except for m-H$_2$BDC, the diacids H$_2$TDC, H$_2$FDC and H$_2$BDC react with Cu ions and form structures with similar architectures. It seems that the exocyclic angle is in fact not very critical in terms of determining the structural architecture of this class of Cu-base coordination polymers.
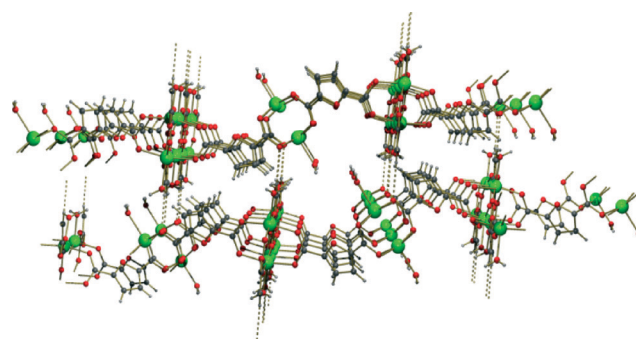

Fig. 1 An asymmetric unit of the crystal structure of Cu-FDC viewed along the crystallographic c-axis. Displacement ellipsoids are drawn at the 50% probability level. Atoms Cu1, O1, and O52 are located on crystallographic mirror planes. Non-coordinated solvent molecules were treated as diffuse electron density (see Experimental section) and were omitted in the drawing. Symmetry operation i: x, $-y$, z.

Fig. 3 Weak C–H···O hydrogen bonding in the crystal structure of Cu-FDC viewed along the crystallographic b-axis. Two-dimensional coordination planes are shown horizontally. Hydrogen bonds are shown as dashed lines.
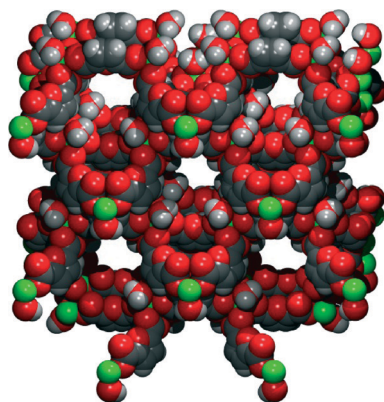
Fig. 4 The space filling plot of the crystal structure of Cu-FDC.

Structural stability

All Cu-samples (Cu-BDC, Cu-TDC, Cu-FDC and Cu-*m*-BDC) were activated to remove the guest solvent molecules (DMF, ethanol and water) occupying the cavities before exploring their hydrogen storage properties. Cu-TDC, Cu-FDC and Cu-*m*-BDC were activated *via* two methods: solvent-exchange (SE, solvents used: CHCl₃ or EtOH) and freeze-drying (FD). Cu-BDC was activated by heating at 225 °C (H225)[14] or by solvent-exchange (EtOH as a solvent). The activated samples were characterized by IR (Fig. S10†), element analysis, thermogravimetric analysis (Fig. S11†) and PXRD (Fig. 5). The TG curves of all four samples reveal that they decompose at about 300 °C (Fig. S10†). The PXRD results show that the structural stability of the resulting coordination polymers is strongly dependent on the activation method used. The

structures of Cu-TDC and Cu-FDC were retained after freeze-drying, which was confirmed by PXRD. However, poor PXRD patterns for Cu-TDC-SE(CHCl₃) and Cu-FDC-SE(CHCl₃) were observed, revealing that CHCl₃-exchange destabilized the Cu-TDC structure and even destroyed the structure of Cu-FDC (Fig. 5A and B). The PXRD results indicate that both CHCl₃-exchange and freeze-drying did not work on the activation of Cu-*m*-BDC. We also tried ethanol as a solvent to activate Cu-*m*-BDC but this appeared unsuccessful as well (Fig. 5C). This suggests that the structure of Cu-*m*-BDC is unstable during the process of removing the guest molecules from the cavities. For Cu-BDC a phase transformation was observed when heated at 225 °C for 22 h, which was confirmed by a different PXRD pattern of Cu-BDC-H225. The structure of Cu-BDC remained intact when the EtOH-exchange method was used (Fig. 5D).

The Cu-TDC and Cu-FDC model structures resulting from single crystal diffraction experiments yield simulated powder diffraction patterns, which show the main reflections and reflection positions that are visible in the powder diffraction pattern of the as prepared samples (Fig. 5A and B). This confirms the structure of the as prepared materials. Deviations in peak intensities of the modeled structures and the experimental ones result from (anisotropic) motions of the linker molecules and from the adsorbed gasses or solvent remaining in the pores. The as measured and simulated XRD patterns for Cu-TDC and Cu-FDC are available in the ESI† in a larger format (Fig. S12).

Hydrogen adsorption

Because Cu-BDC-H225, Cu-BDC-SE(EtOH), Cu-TDC-FD, Cu-FDC-FD and Cu-*m*-BDC-SE(EtOH) form stable structures upon activation, their hydrogen storage properties were investigated on a Sievert's setup at 77 K and below 1.5 bar and the results are shown in Fig. 6 and listed in Table 1. Cu-BDC-H225 showed a hydrogen uptake capacity of 1.22 wt% at 77 K and 1 bar, which is the highest hydrogen uptake among this series. Cu-TDC-FD and Cu-FDC-FD showed hydrogen uptake
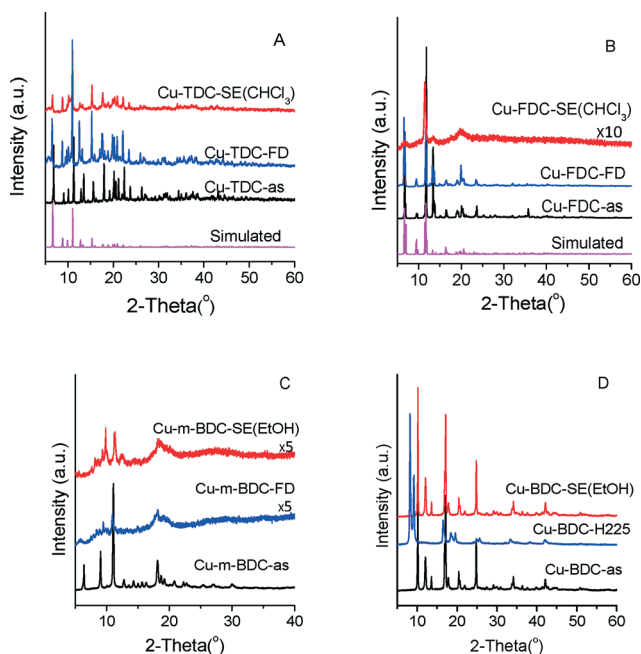

Fig. 5 PXRD patterns of the as prepared and activated Cu-TDC (A), Cu-FDC (B), Cu-*m*-BDC (C) and Cu-BDC (D).
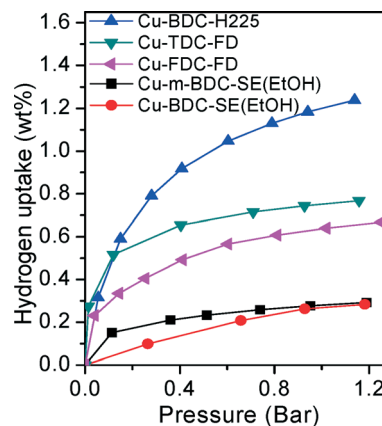

Fig. 6 The low-pressure hydrogen adsorption isotherms of activated Cu-BDC, Cu-TDC, Cu-FDC and Cu-*m*-BDC.

Table 1 The chemical composition, textural properties, H_2 uptake, and isosteric heat of H_2 adsorption of the activated Cu-based coordination polymers

Sample	C (%)	H (%)	N (%)	SSA_{BET} $(m^2\ g^{-1})$	V_p $(cm^3\ g^{-1})$	H_2 uptake[a] (wt%)	Isosteric heat of H_2 adsorption (kJ mol^{-1})
Cu-m-BDC-SE(EtOH)	38.5(41.5)	3.35(2.59)	1.19(2.18)	13	0.03	0.28	3.0
Cu-FDC-FD	36.4(30.6)	3.63(1.69)	4.19(0.00)	310	0.21	0.64	7.5
Cu-TDC-FD	32.9(35.2)	3.10(2.94)	4.10(4.57)	308	0.16	0.75	9.2
Cu-BDC-H225	39.6(47.3)	2.33(3.66)	0.23(4.66)	248	0.17	1.22	7.0
Cu-BDC-SE(EtOH)	n/a	n/a	n/a	8.7	0.01	0.27	2.2

[a] 77 K and 1 bar; The values in brackets are the calculated C-, H-, and N-values based on the structural formula determined by single crystal X-ray diffraction.

capacities of 0.75 wt% and 0.64 wt% at 77 K and 1 bar, respectively. Cu-BDC-ES(EtOH) and Cu-m-BDC-ES(EtOH) displayed comparable hydrogen storage capacities at 77 K and 1 bar (0.27 wt% for Cu-BDC-ES(EtOH) and 0.28 wt% for Cu-m-BDC-ES(EtOH)). The H_2 uptake experiments were repeated 3 times for each sample and the uptake was found to be reversible (Fig. S13†).

The low hydrogen uptake capacities of Cu-m-BDC-SE(EtOH) and Cu-BDC-SE(EtOH) can be explained by their poor porous structures (BET surface area <15 m^2 g^{-1} and pore volume <0.05 cm^3 g^{-1}). The BET surface areas and the pore volumes of Cu-TDC-FD, Cu-FDC-FD and Cu-BDC-H225 are in the range of 248–310 m^2 g^{-1} and 0.16–0.21 cm^3 g^{-1}, respectively (Table 1). A BET surface area of ~300 m^2 g^{-1} has to be considered very low as compared to most other physisorbents used for hydrogen storage applications and indicates a poor porous structure. Compared with MOF-5, which has a BET surface area of ~3000 m^2 g^{-1},[16] the BET surface areas of Cu-BDC-H225, Cu-TDC-FD and Cu-FDC-FD are only one tenth of MOF-5, whereas the hydrogen uptake capacity of Cu-m-BDC-H225 at 77 K and 1 bar is comparable to that of MOF-5 and the hydrogen uptake capacities of Cu-TDC-FD and Cu-FDC-FD at 77 K and 1 bar are about two-thirds that of MOF-5. This indicates that Cu-based metal–organic coordination polymers show a good hydrogen uptake behaviour despite their low surface areas. Moreover, a rapid increase in the hydrogen uptake capacities of Cu-BDC-H225, Cu-TDC-FD and Cu-FDC-FD at low pressures (<0.5 bar) indicates a strong interaction between hydrogen molecules and their respective frameworks. We calculated the isosteric heats of hydrogen adsorption for Cu-BDC-H225, Cu-TDC-FD and Cu-FDC-FD using the Clausius–Clapeyron equation with 0.2 wt% of hydrogen uptake capacity at 77 K and 100 K (Fig. S14†). Isosteric heats of hydrogen adsorption of 7.0, 9.2 and 7.5 kJ mol^{-1} were found for Cu-BDC-H225, Cu-TDC-FD and Cu-FDC-FD, respectively. These values are higher than what is found for most carboxylate-bridged frameworks (3.5–6.5 kJ mol^{-1}) with high surface areas.[17]

Enhancing the isosteric heat of hydrogen adsorption for porous materials is an effective way to improve their hydrogen storage performance under mild conditions at near-room temperature or low pressures. In general, the isosteric heat of hydrogen adsorption can be improved by introducing open metal sites, reducing the pore size and so on.[18] The

presence of open Cu sites can explain the high isosteric heat of hydrogen adsorption for Cu-BDC-H225. Open Cu sites could be formed during the heating step by releasing the coordinating DMF molecules, which is indicated by the lack of a DMF v(CO) band (Fig. S10†). The low nitrogen content of 0.23% (corresponding to 1.2 wt% of DMF) is in agreement with this statement. The theoretical value would be 4.66% and correspond to 24.3 wt% of DMF and is based on the formulae Cu(BDC)(DMF). The low heat of hydrogen adsorption (2.2 kJ mol^{-1}) further substantiates our explanation for Cu-BDC-SE(EtOH), which showed a DMF content of 24.8 wt%, a value comparable to the theoretical calculated value (Fig. S10D†). The high isosteric heats of hydrogen adsorption for Cu-TDC-FD and Cu-FDC-FD cannot be explained by the interaction between hydrogen with open metal sites because there is no evidence of the presence of open copper sites in Cu-TDC-FD and Cu-FDC-FD, as indicated by the presence of nitrogen (N) for Cu-TDC-FD and the high hydrogen (H) content for Cu-FDC-FD (elemental analysis results, Table 1). The pore size is likely to play a determining role in the low-pressure hydrogen adsorption behaviour of Cu-TDC and Cu-FDC. Therefore, the pore sizes of Cu-TDC and Cu-FDC were determined using PLATON.[9] The results reveal that the pore sizes of Cu-TDC and Cu-FDC are mainly in the range of 5.4 Å to 8.0 Å. It is believed that the ideal pore size of porous materials for hydrogen adsorption is 6–7 Å, which results in an optimal interaction between the H_2 molecules and the framework, thus maximizing the total van der Waals forces acting on H_2.[19] Moreover, the isosteric heat of hydrogen adsorption for Cu-TDC is higher than that for Cu-FDC. Considering the different heteroatoms in their structures, we propose that the stronger polarizability of the thiophene ring contributes to the higher isosteric heat of hydrogen adsorption for Cu-TDC. A similar explanation was proposed by the Yaghi group for IRMOF-20 (constructed from thieno[3,2-b]thiophene-1,5-dicarboxylate).[20]

Conclusions

In summary, a series of Cu-based coordination polymers composed of ligands with different exocyclic bond angles were synthesized. The results revealed that the exocyclic bond angle plays only a minor role in the construction of the

structural architecture in this series. Cu-*m*-BDC showed a poor hydrogen uptake capacity because its structure is destabilized during the activation procedure. The all *para*-substituted analogue, Cu-BDC-H225, showed a hydrogen uptake of 1.22 wt% (at 77 K and 1 bar) despite the fact that the framework exhibits a low surface area of 248 $m^2 g^{-1}$. The high isosteric heat of hydrogen adsorption for Cu-BDC-H225 (7.0 kJ mol^{-1}) and high hydrogen uptake can be explained by the presence of open metal sites. The furan and thiophene analogues, *i.e.* Cu-FDC and Cu-TDC, display comparable low surface areas (~300 $m^2 g^{-1}$) and their hydrogen uptake capacities are 0.64 and 0.75 wt% at 77 K and 1 bar. Both coordination polymers display unusually high isosteric heats of hydrogen adsorption, *i.e.* 7.5 and 9.2 kJ mol^{-1} for Cu-FDC and Cu-TDC, respectively. There is no evidence for open metal sites. The high isosteric heats of hydrogen adsorption and the hydrogen uptake can be attributed to an optimal pore size (5.4–8 Å) of the said frameworks and the polarizability of the thiophene and furan building blocks.

Acknowledgements

Notes and references

1 (*a*) S. Kitagawa, R. Kitaura and S. Noro, *Angew. Chem., Int. Ed.*, 2004, **43**, 2334; (*b*) G. Terey, *Chem. Soc. Rev.*, 2008, **37**, 191.

2 M. Eddaoudi, D. B. Moler, H. Li, B. Chen, T. M. Reineke, M. O'Keeffe and O. M. Yaghi, *Acc. Chem. Res.*, 2001, **34**, 319.

3 (*a*) L. J. Murray, M. Dinca and J. R. Long, *Chem. Soc. Rev.*, 2009, **38**, 1294; (*b*) M. B. Lalonde, R. B. Getman, J. Y. Lee, J. M. Roberts, A. A. Sarjeant, K. A. Scheidt, P. A. Georgiev, J. P. Embs, J. Eckert, O. K. Farha, R. Q. Snurr and J. T. Hupp, *CrystEngComm*, 2013, **15**, 9408.

4 (*a*) O. Z. Yesilel, I. Ilker, M. S. Soylu, C. Darcan and Y. Süzen, *Polyhedron*, 2012, **39**, 14; (*b*) Z. Chen, Y. Zuo, X. Li, H. Wang, B. Zhao, W. Shi and P. Cheng, *J. Mol. Struct.*, 2008, **888**, 360;

5 (*c*) P. J. Calderone, D. Banerjee, A. C. Santulli, S. S. Wonga and J. B. Parise, *Inorg. Chim. Acta*, 2011, **378**, 109.

5 Y. H. Hu and L. Zhang, *Adv. Mater.*, 2010, **22**, E117.

6 *Bruker. SAINT-Plus*, Bruker AXS Inc., Madison, Wisconsin, USA, 2001.

7 G. M. Sheldrick, *SADABS and TWINABS: Area-Detector Absorption Correction, v2.10*, Universität Göttingen, Germany, 1999.

8 G. M. Sheldrick, *Acta Cryst.*, 2008, **A64**, 112.

9 A. L. Spek, *Acta Cryst.*, 2009, **D65**, 148.

10 A. J. M. Duisenberg, L. M. J. Kroon-Batenburg and A. M. M. Schreurs, *J. Appl. Crystallogr.*, 2003, **36**, 220.

11 A. M. M. Schreurs, X. Xian and L. M. J. Kroon-Batenburg, *J. Appl. Crystallogr.*, 2010, **43**, 70.

12 M. Eddaoudi, J. Kim, J. B. Wachter, H. K. Chae, M. O'Keeffe and O. M. Yaghi, *J. Am. Chem. Soc.*, 2001, **123**, 4368.

13 M. Eddaoudi, J. Kim, D. Vodak, A. Suidik, J. Wachael, M. O'Keeffe and O. M. Yaghi, *Proc. Natl. Acad. Sci. U. S. A.*, 2002, **99**, 4900.

14 C. G. Carson, K. Hardcastle, J. Schwartz, X. Liu, C. Hoffmann, R. A. Gerhardt and R. Tannenbaum, *Eur. J. Inorg. Chem.*, 2009, 2338.

15 CCDC 956646–956648 contain the supplementary crystallographic data for this paper. These data can be obtained free of charge from The Cambridge Crystallographic Data Centre *via* www.ccdc.cam.ac.uk/data_request/cif.

16 (*a*) M. Sabo, A. Henschel, H. Frode, E. Klemm and S. Kaskel, *J. Mater. Chem.*, 2007, **17**, 3827; (*b*) A. G. Wong-Foy, A. J. Matzger and O. M. Yaghi, *J. Am. Chem. Soc.*, 2006, **128**, 3494.

17 D. Zhao, D. Yuan and H.-C. Zhou, *Energy Environ. Sci.*, 2008, **1**, 222.

18 (*a*) J. L. C. Rowsell and O. M. Yaghi, *Angew. Chem., Int. Ed.*, 2005, **44**, 4670; (*b*) M. Hirscher, B. Panella and B. Schmitz, *MicroporousMesoporous Mater.*, 2010, **129**, 335; (*c*) R. Zou, A. I. Abdel-Fattah, H. Xu, A. Y. Zhao and D. D. Hickmott, *CrystEngComm*, 2010, **12**, 1337.

19 S. Ma and L. Meng, *Pure Appl. Chem.*, 2011, **83**, 167.

20 J. L. C. Rowsell and O. M. Yaghi, *J. Am. Chem. Soc.*, 2006, **128**, 1304.